Original Article

The use of B-scan coupling with A-scan ultrasonography to characterize ocular biometry in canine absolute glaucoma

Napasorn Ngamrojanavanit Natthaporn Tanthasathien Nirachon Srisamai

Suchaya Taotongnuntasin Panrawee Phoomvuthisarn Nalinee Tuntivanich*

Abstract

This study was to investigate intraocular structures of canine absolute glaucomatous eyes using real time B-scan ultrasonography in accordance with the amplitude mode. Ten normal eyes and twenty absolute glaucomatous eyes were included in this study. Ocular biometry via closed-eye technique was performed using the Ultrascan® Imaging System (Alcon Surgical Laboratory, Fort Worth, USA), with a 10 MHz mechanical sector probe. Changes of intraocular structures were descriptively analyzed. Ocular biometry was measured, statistically analyzed and compared between both groups. While mean lens thickness was comparable between normotensive and glaucomatous eyes, mean lens equatorial length was higher in the latter group. Increased hyperechogenicity of lens was ultrasonographically observed in dogs with absolute glaucoma. Axial globe length was significantly greater in the experimental group than the control group ($P<0.05$). In relation to the appearance of the cone-shaped posterior wall, positive correlation between intraocular pressure and axial globe length with statistical significance was noted ($r=0.5$, $P<0.05$). Retinal detachment and lens displacement were also observed in absolute glaucomatous eyes. Not only does ultrasonography, with the 10 MHz frequency transducer, provides ocular biometry to specifically investigate changes of lens and the posterior segment of the canine absolute glaucomatous eyes, it can lead to further selection of appropriate treatment and awareness of post-treatment complications.

Keywords: dogs, glaucoma, ocular biometry, ultrasonography

Department of Veterinary Surgery, Faculty of Veterinary Science, Chulalongkorn University, 39 Henry Dunant Road, Phayathai, Pathumwan, Bangkok, 10330 Thailand

****Correspondence**: nalinee.t@chula.ac.th* (N. Tuntivanich)

Introduction

Glaucoma is one of the most important ocular diseases that lead to permanent loss of vision. A prevalence of dogs suffering from primary breed related glaucoma was reported by Gelatt in 2004 and Storm in 2009. Even though the prevalence of canine glaucoma has not been scientifically reported in Thailand, there has been an increase in the number of canine glaucoma at the Ophthalmology Unit, Animal Teaching Hospital, Faculty of Veterinary Science, Chulalongkorn University, Thailand (personal communication). Glaucoma occurs as a result of aqueous humor accumulation; leading to an increase in intraocular pressure (IOP). Disease progression consists of 3 stages (Gelatt, 2004). The first stage is the early stage with IOPs of 20-30 mmHg. There may be no symptomatic signs or mild changes of pupil, retina and optic disc. If proper treatment has not received, vision will rapidly be threatened. Second is the mild stage with IOPs of 30-40 mmHg. This stage is usually noticeable by suffers from several clinical signs such as episcleral congestion, variable degrees of corneal edema and slight buphthalmos. When IOPs is 40-50 mmHg, the disease has progressed to the advanced stage. Persistent changes associated include corneal edema, mydriasis, optic disc cupping and retinal degeneration.

Ophthalmic signs of glaucoma may be defined as acute and chronic stages, majorly categorized by the duration and progression of the disease. Rapid elevation of IOP is usually observed in the acute stage, which is accompanied by severe pain. The cornea has generalized edema associated with deep vascularization. The pupil is generally constricted. Episcleral congestion is evident. Vision can rapidly be lost within a few hours after IOP elevation. On the other hand, dogs presented with chronic signs of glaucoma can tolerate ocular pain quite well. However, changes of the anatomical structure of the eye in chronic glaucoma are also noteworthy. They include buphthalmos, permanent corneal opacity, lens opacity, intraocular hemorrhage, optic disc cupping and atrophy, generalized retinal degeneration and phthisis bulbi (Renwick, 2002). The atrocious outcome of this whole developing process of glaucoma is an irreversible blindness due to optic neuropathy (Miller and Bently, 2015). Absolute glaucoma will soon occur when the disease has progressed toward the advanced stage. The presence of buphthalmic eyeball will be in accordance with lagophthalmos, keratoconjunctivitis sicca, exposure keratopathy and equatorial staphyloma.

Various diagnostic tools for human glaucoma detection are recommended (Sharma et al., 2008). Though ocular ultrasonography is not one of those, it is widely used to interpret changes within the eyeballs (Dudea, 2011) when direct visualization is inaccessible. It is a technique using high-frequency sound waves travelling through tissue interfaces generating echoes. Each image describes various acoustic characteristic of each tissue. In ophthalmic ultrasonography, a high-frequency transducer within the range of 8-50 MHz is typically used (Millier and Bentley, 2015). Among several types of ultrasonography, amplitude mode (A-mode or A-scan) and brightness mode (B-mode or B-scan) are applicable in animals. A-scan ultrasonography offers a one-dimensional display of echoes in a spike pattern. Time delay is required for sound waves to reach given ocular tissue interfaces. The height of spikes describes strength of echoes. The indication of an A-scan ultrasonogram is therefore to measure distance between ocular interfaces. B-scan ultrasonography represents two-dimensional image receiving from an oscillating wave that passes through a cross-section of tissues. The great advantage of B-mode ultrasonography is to observe the intraocular contents of the globe, obscured by ocular media opacity. Intraocular neoplasm, intraocular inflammation, retinal detachment and vitreous hemorrhage are good suggestion for ultrasonographic investigation in cases with opaque ocular media (Gallhoefer et al., 2013).

According to the fact that the ocular media of dogs with absolute glaucoma is obscured from examination, ultrasonography is therefore considered an applicable diagnostic tool to evaluate anatomical changes within glaucomatous eyes (Aldavood et al., 2012). Our objective was to characterize ocular biometry in canine absolute glaucoma with the use of B-scan coupling with A-scan ultrasonography.

Materials and Methods

***Samples*:** A total of thirty eye balls from thirty small-breed dogs weighing not more than 10 kilograms were included into the study. These dogs were presented at the Ophthalmology Unit, Small Animal Teaching Hospital, Faculty of Veterinary Science, Chulalongkorn University. All procedures were performed under informed consent provided by the owners of all dogs. All procedures had been approved by the Chulalongkorn University Animal Care and Use Committee with approved Animal Use Protocol number 1731024, and care was taken to comply with the 3R concept.

Eyes were divided into 2 groups; controls and experiments. There were 10 randomized control eyes (from 10 dogs) with IOP ranging from 5-20 mmHg in a control group. Ophthalmic examinations revealed no intraocular inflammation, corneal disorders of systemic diseases that affect intraocular pressure. There were twenty randomized eyes in the experimental group. They were from twenty dogs diagnosed with advanced/absolute glaucoma. They had a history of IOP more than 35 mmHg. The disease had been progressing for not less than 3 months duration. All dogs were on ocular hypotensive medications.

***Procedures*:** All procedures had been approved by the Chulalongkorn University Animal Care and Use Committee with approved Animal Use Protocol number 1731024, and care was taken to comply with the 3R concept.

To categorize dogs into control and experimental groups, they underwent general ophthalmic examinations. Examinations included (1) Schirmer tear test I, (2) neuro ophthalmic reflexes: menace response, dazzle reflex and pupillary light response, (3)

fluorescein staining test (4) rebound tonometry; a measurement of intraocular pressure using the Tonovet® (Tiolat Oy, Helsinki, Finland), (5) dark/light room direct eye examination, and (6) assessment of the anterior chamber using a slit lamp biomicroscope (Kowa SL-15; Kowa company, Ltd, Japan).

Ocular ultrasonography was performed through the eyelid in all awakened dogs by an experienced veterinarian. Interobserver variability was then minimized. Intra-observer reliability was still maintained by using an automated optical axis together with visual axis as an indicator of all measurements. Ultrasonographic images were obtained from a B-mode ultrasonogram coupling with amplitude spikes (single A&B mode), with the use of the Ultrascan® Imaging System (Alcon Surgical Laboratory, Fort Worth, USA). The transducer probe was 10 MHz mechanical sector. A topical 0.5% tetracaine hydrochloride was applied to the cornea at a dose of 2 drops within 3-minute interval times. All dogs were gently handled with minimal restraint and the transducer probe with acoustic coupling gel was perpendicular to the center of the cornea. The probe position marker was always placed in the rostral to caudal direction. Once parallel plane to visual axis was achieved, an oblique plan was performed to observe intraocular architectures. Immediately after the procedure was finished, the acoustic coupling gel was flushed off to ensure the safety of the ocular surface. Ultrasonographic images were recorded for further analysis.

***Data collection and data analysis*:** There were two major parts of data interpretation.

1. Structural abnormalities detected by B-mode ultrasonograms were categorized and descriptively analyzed.

2. Measurement of length/depth of intraocular structures from ultrasonographic images: A measurements were performed by Adobe Photoshop CC 2017 (©Adobe System, Inc., San Jose, USA). Each location from B-mode image was in accordance with the amplitude spike.

2.1 Anterior chamber depth (ACD): ACD was measured from the corneal epithelium to the anterior lens capsule.

2.2 Lens thickness (LT): LT was measured from the axial point of the anterior to the posterior lens capsule.

2.3 lens equatorial length (LEL): LEL was measured from equator to equator of the lens.

2.4 Vitreous chamber depth (VCD): VCD was measured from the axial point of the posterior lens capsule to the fundus.

2.5 Axial globe length (AXL): AXL was measured from the corneal epithelium to the fundus.

Means (± SD) of each measurement from both groups were calculated. Comparisons of means between control and experimental groups, using independent t-test (SPSS program version 22.0, IBM Corporation, NY, USA) at a significance level of $p<0.05$. Pearson's correlation test (SPSS program version 22.0, IBM Corporation, NY, USA) was applied to evaluate the correlation between intraocular pressure and five parameters. Statistical significance was considered when $p<0.05$.

Results

Clinical demographic data of all patients is in Table 1. Experimental eyes had IOP ranging from 31 to 63 mmHg.

In the control group (Fig 1), the cornea was identified as a curved hyperechoic interface immediately parallel to the eyelid. The anterior chamber was indicated as anechoic cavity between two hyperechoic structures; corneal endothelium and anterior lens capsule. The lens appeared as an elliptical anechoic structure with hyperechoic anterior and posterior lens capsule. The vitreous chamber was in a spherical shape. It was occupied with anechoic materials. The posterior wall was revealed as a hyperechoic curvilinear structure at the back of the eyeball.

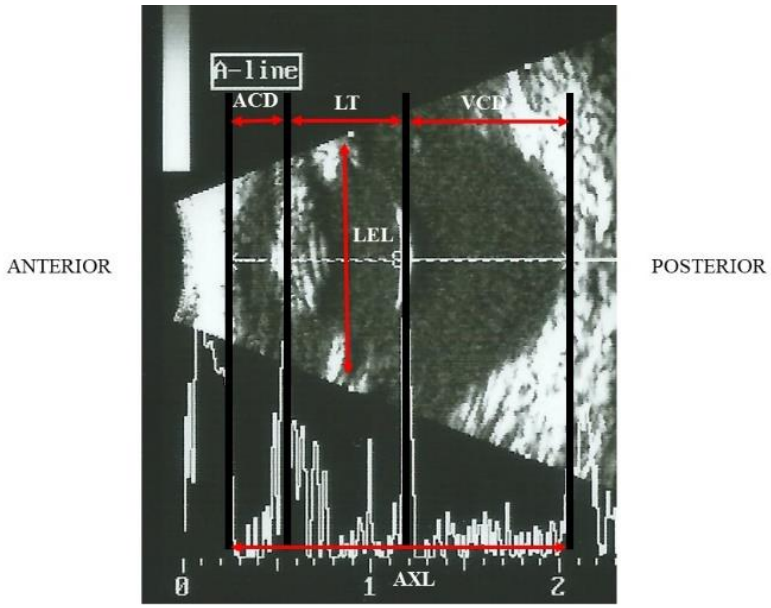

Figure 1 Representative ultrasonographic image of a normal eye, along with measurements; anterior chamber depth (ACD), lens thickness (LT), lens equatorial length (LEL), vitreous chamber depth (VCD), and axial globe length (AXL).

Various ocular abnormalities were identified in glaucomatous eyes (Table 2). Partial hyperechoic homogenous material was evident in the anterior chamber (8/20; 40%) (Fig 2A). Fine dispersed opacity was ultrasonographically noticed in the anterior chamber of two out of ten control eyes (20%). Ten experimental eyes were hyperechoic (50%) (Fig 2B). Increased echogenicity was noticed in lens capsules which had apparent hyperechoic lens materials. In controls, lens materials were hyperechoic in three out of ten (30%) eyes. Displacement of lens was evident in five out of twenty eyes (25%). Most of the echoic lens were luxated to the ventral/posterior of the eyeballs (Fig 2C). Mild to moderate intensities of echoic homogeneous materials were observed in the vitreous chamber of the glaucomatous eyes (5/20; 20%) (Fig 2D). Retinal detachment appeared as the v-y structure of a linear echoic membrane projecting in front of the posterior wall. Of 20 eyes, three (15%) retinal detachments were detected (Fig 2E). Obvious cone-shaped posterior wall was identified in eight out of 20 (40%) in glaucomatous eyes (Fig 2F).

Table 1 Clinical demographic data of all patients involved in this study.

Dog	Gender	Age (years)	Breed	Side of eye	Averaged IOP (mmHg)
1	Female	3	Chihuahua	OS	13
2	Male	10	Mixed	OS	11
3	Female	8	Mixed	OD	11
4	Male	10	Shih Tzu	OS	8
5	Male	9	Mixed	OS	10
6	Male	10	Shih Tzu	OD	8
7	Female	8	Mixed	OS	12
8	Female	2	Mixed	OD	9
9	Female	8	Chihuahua	OD	9
10	Female	13	Shih Tzu	OS	9
11	Female	7	Mixed	OS	32
12	Male	10	Mixed	OS	33
13	Male	11	Mixed	OD	44
14	Male	10	Poodle	OD	31
15	Female	11	Shih Tzu	OS	63
16	Female	2	Mixed	OS	60
17	Female	13	Shih Tzu	OD	37
18	Female	12	Poodle	OD	49
19	Female	13	Shih Tzu	OS	45
20	Female	10	Shih Tzu	OS	41
21	Male	13	Mixed	OS	40
22	Female	9	Shih Tzu	OS	60

*Dog 1-10 = control group, Dog 11-30 = experimental group

Table 2 Ocular abnormalities identified by ultrasonography.

Ocular abnormality	Number of eyes (total of 20)
Hypoechogenic homogenous materials filling in the anterior chamber	8
Hyperechoic lens materials	10
Displaced echoic lens in the vitreous chamber	5
Multiple point-liked echoic foci in the vitreous chamber	5
Hyperechoic membrane pointing from the posterior wall into vitreous chamber	3
Hyperechoic cone-shaped posterior wall of the eye	8

Comparison of the two chambers between the experimental group and controls revealed different mean depth (Fig 3). Both mean anterior and vitreous chamber depths of glaucomatous eyes were higher than those of the controls. Statistically, significant difference was noted in the vitreous chamber depth. There was a low degree of positive correlation between vitreous chamber depth and IOP without statistical significance (r=0.461; $p>0.05$). Slight changes of lens thickness and lens equatorial length is shown in figure 4. As compared to the controls, the mean lens equatorial length of the glaucoma group was longer, whereas the mean lens thickness was shorter (6.26±0.57 mm). A low degree of positive correlation was noted between lens thickness and IOP without statistical significance (r=0.308; $p>0.05$).

Mean axial globe length in glaucomatous eyes was significantly longer (20.36±3.01 mm), compared to that of control eyes (16.49±0.82 mm) (Fig 5). It had a moderate positive correlation to IOP with statistical significance (R=0.68; $p<0.05$) (Fig 6). There was no statistical correlation between IOP and anterior chamber depth (r=-0.135; $p>0.05$) as well as lens equatorial length (r=0.049; $p>0.05$).

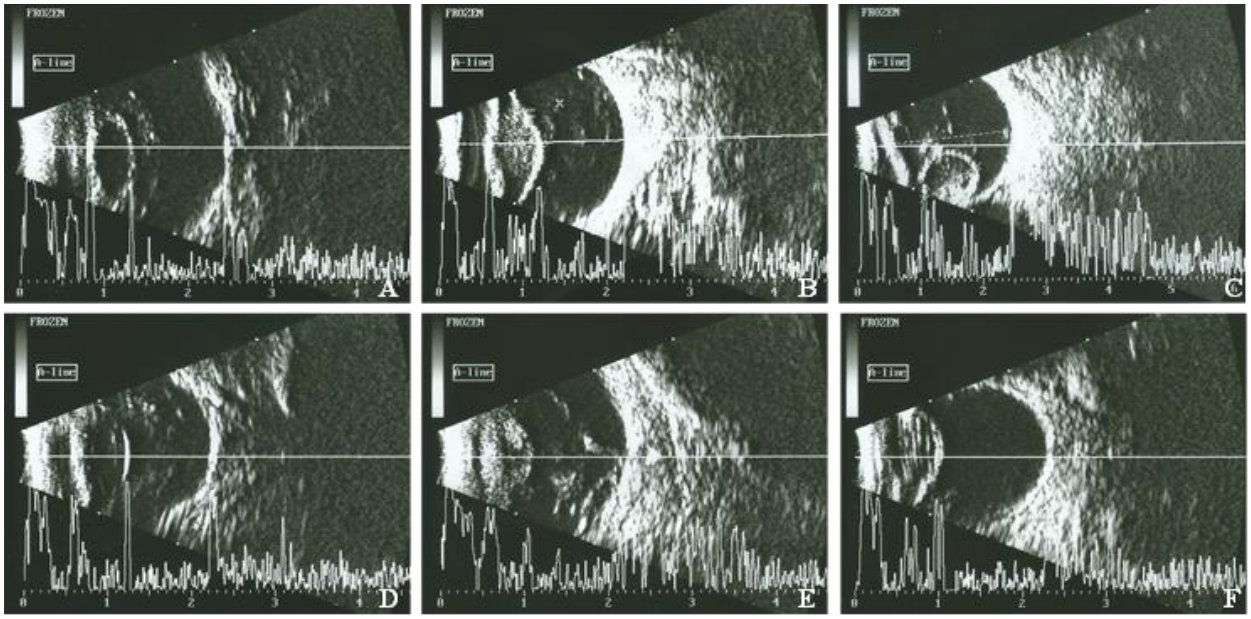

Figure 2 Ultrasonographic images from absolute glaucomatous eyes demonstrated (2A) hypoechoic homogenous material filling the anterior chamber, (2B) hyperechoic lens materials, (2C) displaced spherical echoic lens into vitreous chamber, (2D) multiple point-liked echoic foci in the vitreous chamber, (2E) hyperechoic membrane pointing from the posterior wall into the vitreous chamber and (2F) hyperechoic cone-shaped posterior wall.

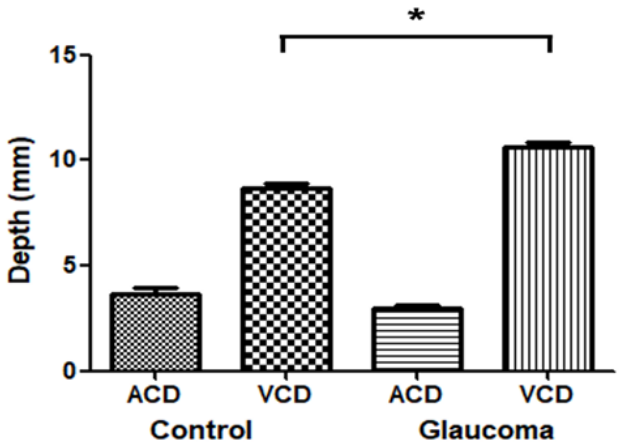

Figure 3 Mean (±SD) of the anterior chamber depth (ACD) and vitreous chamber depth (VCD) of the control and experimental groups. Star (*) indicates statistical significance at a level of $p < 0.05$.

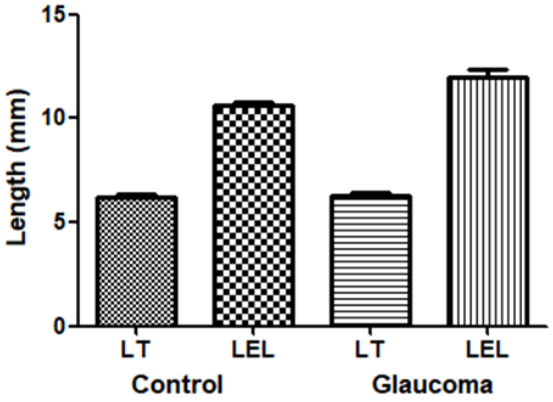

Figure 4 Mean (±SD) of the lens equatorial length (LEL) and lens thickness (LT) of the control and experimental groups.

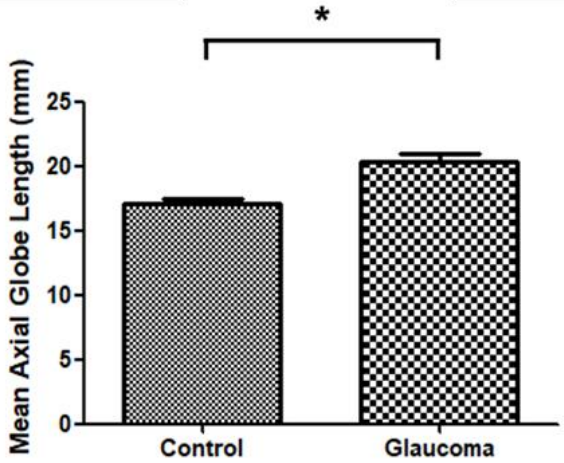

Figure 5 Mean (±SD) of the axial globe length of the control and experimental group. Star (*) indicates statistical significance at a level of $p < 0.05$.

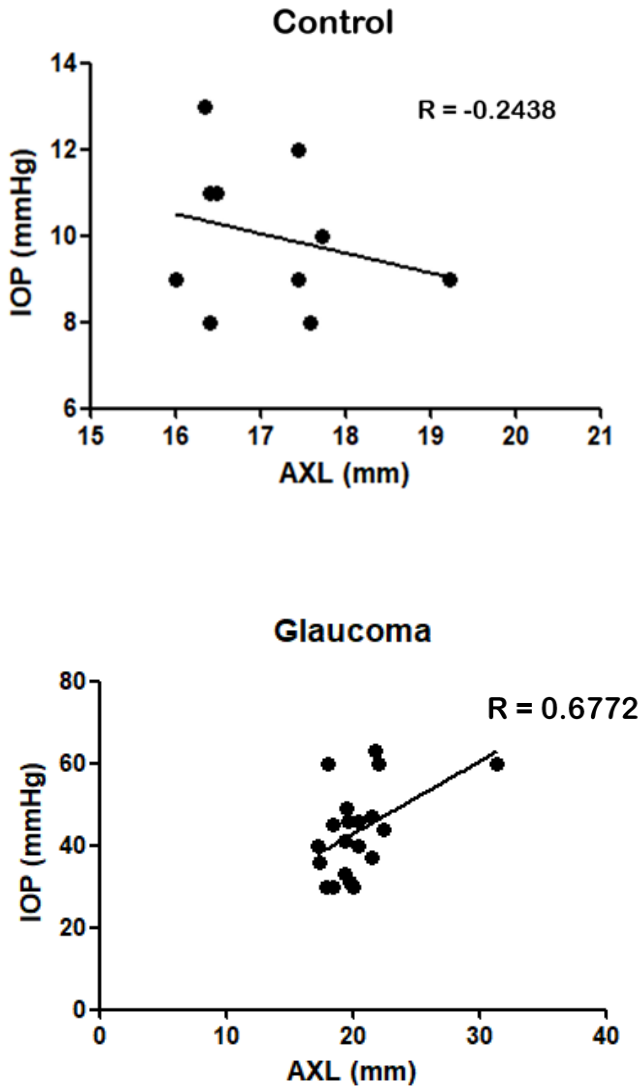

Figure 6 Correlation between intraocular pressure (IOP) and axial globe length (AXL) of the control and experimental groups. Star (*) indicates statistical significance at a level of $p < 0.05$.

Discussion

B-mode ultrasonography provides good investigation through opaque ocular media in absolute glaucomatous eyes. Good animal restraint is required to perform ocular ultrasonography. Rotation of eyeballs away from the visual axis may result in incorrect assessment (Squarzoni et al.,2010); particularly length or depth measurements. In our study, we attempted to collect only ultrasonograms where the optical axis is perpendicular among the cornea, lens surface and the posterior wall. Amplitude of spikes coupling with B scan was used (Cottrill et al., 1989; Hamidzada, 1999) as guidance for all measurements of ocular biometry. To ensure proper data interpretation, one investigator was assigned to measure ultrasonographic images presented via commercialized imaging software program.

A cone-shaped posterior wall is a substantial consequence of long-term pressure in chronic glaucoma. It is presented as globe elongation that could lead to lens displacement. A significant increase of mean vitreous chamber depth (He et al., 2012) and mean axial globe length is related to axial globe elongation in glaucomatous eyes (Cho, 2008). Positive correlation between mean axial globe length and IOP in glaucoma was not only found in our study but also reported in normotensive marmoset (Nickla et al., 2002) and chicken (Schmid et al., 2003). Their mean axial globe length increases at night when diurnal IOP is the highest. With time of glaucoma progression to advanced stage, cupped disc due to loss of myelin and prominent lamina cribrosa atrophy may be part of the reason for the longer depth of the mean vitreous chamber and axial globe length. Appearance of scattered hyperechoic materials in the vitreous chamber, likely indicates vitreous degeneration or inflammatory cell dispersion, rather than vitreous hemorrhage.

Loss of lens transparency, due to the increase of lens protein insolubility, ultrasonographically reflects hyperechoic materials within the lens cortex and nucleus, clinically described as cataract formation (Michael and Bron, 2011). Though aging can cause degenerative changes of lens fiber observed in some of our control dogs mostly at middle age, prominent interlenticular density was found in the glaucomatous group a the median age of 10 years. At the stage of liquefactive lens degeneration, while there was a slightly lower mean lens thickness due to lens resorption in advanced glaucoma long-term extension of zonular fibers from globe enlargement caused longer mean lens equatorial length. Our finding is contrary to a study in patients with occludable open-angled glaucoma (George et al., 2003) where lens thickness increased. Their patients were in middle age, when the water imbibition mechanism is supposely active during an early stage of cataract formation.

Regardless of a clear anterior chamber ophthalmoscopically examined in controls, our study reveals hypoechoic appearance within the anterior chamber in both groups. We speculate that this artifact is because of insufficient resolution (Guhu et al., 2006) due to low ultrasonic frequency of 10 MHz. In fact, ultrasound biometry is known for better interpretation of the posterior segment of the eye. With the use of 10-15 MHz to assess anterior ocular segment, enough coupling gel (MacKay and Mattoon, 2015) or a standoff (Gonzalez et al., 2001) is recommended via a closed-eye technique to avoid ultrasonographic artifacts. Nevertheless, the presence of hypoechoic material within the anterior chamber of glaucomatous eyes may indicate real pathological incidence related to the replacement of hyaluronic acid by fibronectin and thrombospondin in glaucoma patients (Gabelt and Kaufman, 2005). In terms of depth, it is likely to find a decrease of the anterior chamber depth, as a result of anterior lens displacement (Cho et al., 2002). The increase in corneal thickness (Muir et al., 2004) as well as positive correlation between IOP and central corneal thickness in dogs (Park et al., 2011) may cause insignificant comparison of the anterior chamber depth in our study. For better interpretation of the anterior segment, ultrasound biomicroscopy providing high frequency of 35-50 MHz is recommended (Bently et al., 2003).

In conclusion, ocular biometry of canine absolute glaucoma could be characterized with the use of B-scan coupling with A-scan ultrasonography. With additional apparent peaks of A scan, determination of ocular organs could be more precise and accurate. Several pathological changes were apparently associated with chronic increased intraocular pressure. Assessment of intraocular structures could therefore be beneficial for further surgical therapy, as well as long-term treatment of the disease complications.

Conflict of interest: The authors declare no conflict of interest in the study.

Acknowledgements

The study was funded by the senior project grant for veterinary students, Faculty of Veterinary Science, Chulalongkorn University. We would like to acknowledge the staff of the Ophthalmology Unit, Small Animal Teaching Hospital, Faculty of Veterinary Science, Chulalongkorn University for their assistance and support.

References

Aldavood SJ, Zahedi R, Sohrabi Haghdoost I, Rezaie Kanooy M and Veshkini A 2012. Ultrasonographic findings of experimental glaucoma in rabbits. Comp Clin Path. 22(4): 585-589.

Bentley E, Miller PE and Diehl KA 2003. Use of high-resolution ultrasound as a diagnostic tool in veterinary ophthalmology. J Am Vet Med Asso. 223(11): 1617-1622.

Cho HJ, Woo JM and Yang KJ 2002. Ultrasound biomicroscopic dimensions of the anterior chamber in angle-closure glaucoma patients. Korean J Ophthalmol. 16: 20-25.

Cho YK 2008. Early intraocular pressure and anterior chamber depth changes after phacoemulsification and intraocular lens implantation in nonglaucomatous eyes. Comparison of groups stratified by axial length. J Cataract Refract Surg. 34(7): 1104-1109.

Cottrill NB, Banks WJ, Pechman RD 1989. Ultrasonographic and bio- metric evaluation of the eye and orbit of dogs. Am J Vet Res. 50(6): 898–903.

Dudea SM 2011. Ultrasonography of the eye and orbit. Medical Ultrasonography. 13(2): 171-174.

Gabelt BT and Kaufman PL 2005. Changes in aqueous humor dynamics with age and glaucoma. Prog Retin Eye Res. 24(5): 612-637.

Gallhoefer NS, Bentley E, Ruetten M, Grest P, Haessig M, Kircher PR, Dubielzig RR, Spiess BN and Pot SA 2013. Comparison of ultrasonography and histologic examination for identification of ocular diseases of animals: 113 cases (2000-2010). J Am Vet Med Assoc. 243(3): 376-388.

Gelatt KN and MacKay EO 2004. Prevalence of the breed related glaucoma in pure-bred dogs in North America. Vet Ophthalmol. 7(2): 97-111.

George R, Paul PG, Baskaran M, Ramesh SV, Raju P, Arvind H, McCarty C and Vijaya L 2003. Ocular biometry in occludable angles and angle closure glaucoma: a population-based survey. Br J Ophthalmol. 87: 399-402.

Gonzalez EM, Rodriguez A and Garcia I 2001. Review of ocular ultrasonography. Vet Radiol Ultrasoun. 42(6): 485-495.

Guhu S, Bhende M, Baskaran M and Sharma T 2006. Role of ultrasound biomicroscopy in the detection and localisation of anterior segment foreign body. Ann Acad Med Singafore. 35: 536-540.

Hamidzada WA 1999. Agreeement between A-mode and B-mode ultralsonography in the measurement of ocular distances. Radiology and Ultrasound. 40(4): 502-507.

He L, Wendt M and Glasser A 2012. Manipulation of intraocular pressure for studying the effects on accommodation. Exp Eye Res. 102 : 76-84.

MacKay CS and Mattoon JS 2015. Eye. In: Small Animal Diagnostic Ultrasound. 3 ed. John S Mattoon and

Thomas G Nyland (eds). Missouri: Elsevier Saunders. 128-154.

Michael R and Bron AJ 2011. The aging lens and cataract: a model of normal and pathological ageing. Philos Trans R Soc Lond B Biol Sci. 366(1568) : 1278-1292.

Miller PE and Bentley E 2015. Clinical Signs and Diagnosis of the Canine Primary Glaucomas. Vet Clin North Am Small Anim Pract. 45(6): 1183-1212.

Muir KW, Jin J and Freedman SF 2004. Central corneal thickness and its relationship to intraocular pressure in children. Ophthalmology. 111(12): 2220-2223.

Nickla DL, Wildsoet CF and Troilo D 2002. Diurnal Rhythms in Intraocular Pressure, Axial Length, and Choroidal Thickness in a Primate Model of Eye Growth, the Common Marmoset. Invest Opthalmol Vis Sci. 48(8): 2519-2528.

Park Y-W, Jeoung M-B, Kim T-H, Ahn J-S, Ahn J-T, Park S-A, Kim S-E and Seo K 2011. Effect of central corneal thickness on intraocular pressure with therebound tonometer and the applanation tonometer in normal dogs. Vet Ophthalmol. 14(3): 169-173.

Renwick P 2002. Glaucoma. In: BSAVA Manual of Small Animal Ophthalmology. 2nd ed. Gloucester: BSAVA 185-203.

Schmid KL, Hills T, Abbott M, Humphries A, Pyne K and Wildsoet CF 2003. Relationship between intraocular pressure and eye growth in chick. Ophthal Physiol Opt. 23: 25-33.

Sharma P, Sample PA, Zangwill LM, and Schuman JS 2008. Diagnostic Tools for Glaucoma Detection and Management. Surv Ophthalmol. 53 (SUPPL1): 17-32.

Squarzoni R, Perlmann E, Antunes A, Milanelo L and Barros PSdM 2010. Ultrasonographic aspect and biometry of Stripped owl's eyes (Rhinoptynx clamator). Vet Ophthalmol. 13(1): 86-90.